Development of novel anti-angiogenic SRPK1 inhibitors

Jennifer Batson[1], Claire Allen[1], J. Zhang[2], Stephen Wearmouth[2], Jonathan Morris[2], Melissa Gammons[3], David Bates[1,3]

[1]Cancer Biology, Division of Cancer and Stem Cells, University of Nottingham, Queen's Medical Centre, Nottingham NG2 7UH, [2]School of Chemistry, University of New South Wales, Sydney,[3]Microvascular Research Laboratories, University of Bristol.

The University of Nottingham

UNITED KINGDOM · CHINA · MALAYSIA

Introduction

Angiogenesis, the formation of new blood vessels from existing vasculature, underlies disease progression in a range of conditions including wet age-related macular degeneration (wAMD) and cancer (Figure 1). Most anti-angiogenic therapies target VEGF or its receptors; the principal signalling pathway that drives physiological blood vessel formation during development and deregulated, uncontrolled blood vessel formation during disease. However, current anti-angiogenic therapies are associated with limited efficacy, non-specific effects, resistance and toxicity[1].

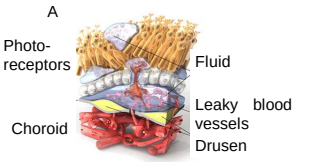

Diagram 1. (A) In wAMD, VEGF-A production promotes choroidal neovascularisation. Accumulation of fluid and bleeding causes central vision loss and if left untreated and scar tissue develops, vision loss is permanent. (B) Tumour cells and supporting cells release VEGF which promotes angiogenesis to nourish the tumour with nutrient from the blood and provide an escape route for metastasis.

VEGF-A mRNA is alternatively spliced into two isoforms with distinct functions; pro-angiogenic VEGF-A_{165}a and anti-angiogenic, cytoprotective VEGF-A_{165}b[2] (Figure 2).

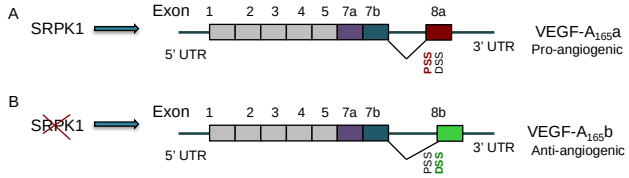

Diagram 2. Schematic diagram to show alternative slicing of VEGF-A mRNA in exon 8. (A) SRPK1-mediated proximal splice site selection in exon 8 leads to selection of exon 8a, generating pro-angiogenic VEGF-A_{165}a. (B) Inhibition of SRPK1 leads to distal splice site selection in exon 8, selection of exon 8b and production of anti-angiogenic VEGF-A_{165}b.

SRPK1 inhibitors

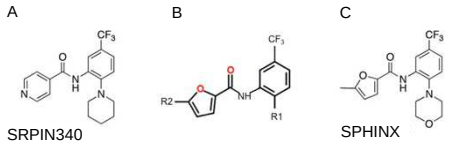

Figure 1. Structures of SRPIN340 (A), and SPHINX compounds. The latter are low molecular weight (around 500 Da), disubstituted furan structures. The generic SPHINX structure is shown (B), from which novel compounds were designed through medicinal chemistry with modified R1 and R2 groups. The structure of SPHINX is shown (C) (adapted from Gammons et al., 2013)

SPHINX compounds inhibit SRPK1 kinase activity in vitro

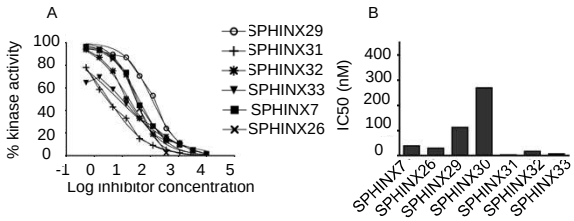

Figure 2. Novel compounds inhibit SRPK1 kinase activity in vitro. SRPK1 activity was tested using a Kinase-Glo assay with the purified SRPK1 protein, the RS peptide of SRSF1 and ATP (A). Compounds dose-dependently inhibited SRPK1 kinase activity. IC50s of the various compounds (B).

hERG inhibition with SPHINX compounds

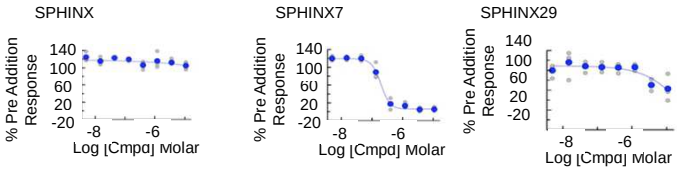

Figure 4. hERG inhibition profiles of lead compounds. SPHINX does not significantly inhibit hERG (IC50<11μM) but SPHINX7 does (IC50 0.2μM). Our medicinal chemistry approach developed SPHINX29, which does not significantly inhibit hERG and SPHINX31, which does inhibit hERG with and IC50 of 0.3μM but this is 100x higher than its IC50 of SRPK1 inhibition

SPHINX compound salts inhibit SRPK1 kinase activity in vitro

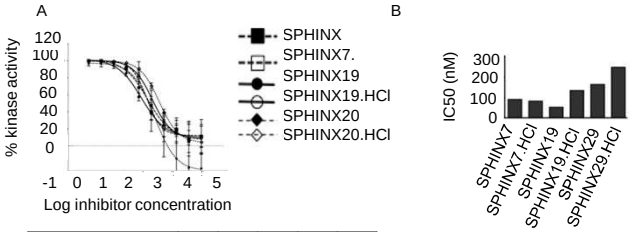

Compound	1.00	0.50	0.25	0.13	0.06
SRPIN340					
SPHINX7.HCl. pH 7					
SPHINX7 dH2O					

Figure 3. Novel compound HCl salts inhibit SRPK1 activity in vitro. SPHINX compound HCl salts dose-dependently inhibited SRPK1 kinase activity as efficiently as unconjugated SPHINX compounds (A). IC50s of the compounds (B). HCl salt conjugates were more soluble than unconjugated SPHINX compounds (C).

Proliferation following SPHINX compound treatment

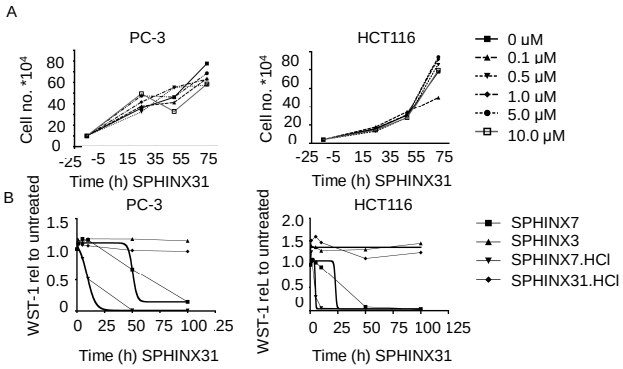

Figure 5. (A) Proliferation was assessed by manually counting cells at 0 h, 24 h, 48 h and 72 h after administration of SPHINX31 or (B) by a WST-1 assay to measure cell metabolism after treatment with SPHINX7, SPHINX31 SPHINX7.HCl or SPHINX31.HCl.

SPHINX compounds inhibit laser-induced CNV in vivo

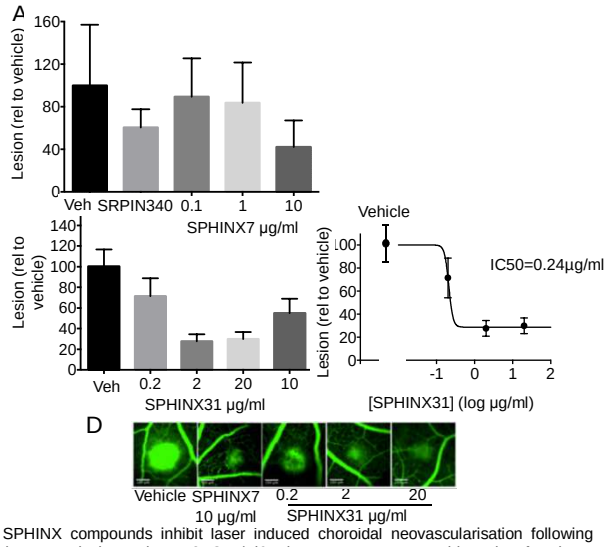

Figure 6. SPHINX compounds inhibit laser induced choroidal neovascularisation following administration as topical eye drops. 3. C57/Bl6 mice per group were subjected to four laser (lesions to the back of the eye on day 0. From day 1 to 14 mice received twice daily topical treatments of A) SPHINX7 or SRPIN340, or B) SPHINX31 at concentrations shown. Lesions were imaged by A) staining of retinas for choroidal neovascularisation, or B) fluorescein angiography. C. Dose response to SPHINX31. IC50 =1.84μM (~1μg/ml). D. Example images of fluorescein angiography showing representative lesion sizes.

References

1. Carmeliet et al., Nature 2013
2. Bates et al., Cancer Research 2002
3. Gammons et al., Invest Opthalmol Vis Sci 2013

Acknowledgements

This work was funded by a University of Nottingham Hermes grant.